Hydraulic transient analysis and leak detection on transmission pipelines: field tests, model calibration and inverse modelling

by

Stephens, M.L., Simpson, A.R. and Lambert, M.F.

9th Annual Symposium on Water Distribution Systems Analysis

Citation:
Stephens, M.L., Simpson, A.R. and Lambert, M.F., (2007) "Hydraulic transient analysis and leak detection on transmission pipelines: field tests, model calibration and inverse modelling", *9th Annual Symposium on Water Distribution Systems Analysis*, American Society of Civil Engineers, Tampa, Florida, USA, 15-19 May.

For further information about this paper please email Angus Simpson at angus.simpson@adelaide.edu.au

HYDRAULIC TRANSIENT ANALYSIS AND LEAK DETECTION ON TRANSMISSION PIPELINES : FIELD TESTS, MODEL CALIBRATION AND INVERSE MODELLING

Mark L. Stephens, Angus R. Simpson and Martin F. Lambert
The University of Adelaide
Adelaide, South Australia (Australia)
mstephen@civeng.adelaide.edu.au, asimpson@civeng.adelaide.edu.au,
mlambert@civeng.adelaide.edu.au

Abstract

The use of hydraulic transients for leak detection is theoretically possible assuming that water pipelines respond elastically and that current transient models are capable of replicating measured responses from real pipelines. This paper presents results for tests using hydraulic transients with and without a leak on a typical transmission main in South Australia. The size of the leak artificially introduced to the pipeline was set at the maximum limit of interest to South Australian Water Corporation operators.

Based on the results of the field tests and modelling performed using a quasi-steady friction transient numerical model it was found that it was difficult to model the response of the pipeline, without and with the introduced leak, because of unsteady friction and mechanical dispersion and damping of the transient waveforms. Inverse analysis was performed using the quasi-steady friction transient model and it was found that leak could not be successfully detected. The transient model was improved by including unsteady friction and a "viscous" damping mechanism that was calibrated for inelastic mechanical effects using no-leak measured responses.

Inverse transient analysis was performed using this improved model focussed on reflection information over 2L/a seconds of the measured leak responses and over an extended period. The small size of the direct reflections from the artificial leak made them difficult to discern amongst other reflections from elements not related to the leak. The inverse transient analysis performed over an extended period made use of leak damping information but was also affected by sources of damping not related to the leak. It was found that the improved forward transient model, in combination with prior information regarding the leak discharge (commonly available for flow monitored transmission pipelines), gave the best estimate of the location and size of the leak. However, the "true" leak was not identified as the optimal candidate following the inverse transient analysis because of persistent inadequacies in the replication of all the physical complexities affecting the measured transient responses.

Keywords
Hydraulic transients, Leaks, Detection, Inverse Analysis

1. INTRODUCTION

Leakage from water pipelines is a serious problem that has been the focus of both regulatory and technological changes and developments since the early 1990s. One of the technological developments that has received considerable research interest is the

use of artificially generated transients (i.e., small water hammer events), and inverse techniques to interpret the measured response of water pipeline systems, to diagnose leakage. The concept of using inverse transients for the diagnosis of leaks was first numerically demonstrated by Liggett and Chen (1994).

While the interpretation of a transient response to diagnose a leak is theoretically possible, assuming that water pipelines respond elastically and that current transient models are capable of replicating measured responses from field pipelines, results presented by Covas et al. (2006) and in this paper confirm that modelling the response of field pipelines over an extended period is complicated by physical uncertainties. Typically, these complexities have less impact over the first 2L/a seconds of the transient response of a pipeline (the return time for the water hammer wave) and Covas et al. (2006) focussed on this information. However, the inability to accurately model responses over an extended period places reliance on the information contained in the initial leak reflection and prevents the use of leak damping information to diagnose the leak. If the leak reflection is difficult to discern, due to significant reflections from other physical complexities complicating the measured responses, reliance on the reflection information becomes problematic.

Improvements to the forward transient model are presented in this paper to enable interpretation of extended period damping information within the measured responses. Results are presented for techniques that both do not and do require calibration to no-leak responses. The results of the field investigation and inverse transient analysis are used to confirm the importance of direct leak reflection information. The added benefit of being able to interpret the extended period damping information is also demonstrated. The field results can be used, with those presented by Covas et al. (2006), to appraise the practicality of using artificial hydraulic transients, and inverse techniques to interpret measured responses, for the diagnosis of leaks on field pipelines.

2. REFLECTION AND DAMPING INFORMATION

When transient waves arrive at a leak location a loss of energy occurs coupled with a reflected wave. The size of the reflected wave is proportional to both the size of the leak and transient overpressure. If the reflected wave is large, relative to other reflections and the dispersion and damping from, amongst other things, fluid structure interaction, inelastic damping, joints and internal fluid effects, it will persist for 2L/a, 4L/a or longer and may be usefully interpreted as direct reflection information. However, if the leak is small then the direct reflection information will be less distinct and may be obscured by other sources of dispersion and damping. Furthermore, the interpretation of direct leak reflection information may be confused when other sources of distinct reflections exist within a pipeline (e.g., lateral pipe connections, joints and air pockets). Nevertheless, energy is removed by the leak with each pass of the transient wave, despite the fact that direct reflections are imperceptible, and this energy loss manifests as damping information where the damping simply equates to the effect from indistinct leak reflections.

A precise understanding of other sources of dispersion and damping in a pipeline is required if the damping contribution from a relatively small leak, with indistinct direct reflections, is to be isolated. For example, effects from unsteady friction, fluid

structure interaction, mechanical movement, roughness, joints and air pockets can all cause dispersion and damping. If these effects cannot be precisely included in a model, or calibrated using a no-leak response, then a leak cannot be accurately identified using damping information. In this context, the availability of prior information, for example, knowledge of the leak discharge, may supplement the damping information and partially compensate for an imprecise model. This information is often available for trunk transmission pipelines that are flow monitored (as was the pipeline investigated in this paper).

3. INVESTIGATION OF FIELD TRANSMISSION PIPELINE

3.1 Details of South Australian Water Corporation pipeline and tests

The Hanson Transmission Pipeline (HTP) is located near the township of Hanson, in the mid-north region of South Australia, and is approximately 13.5 km long by 650 mm nominal diameter. It was subject to artificial transient tests on the 21st May 2004 and was selected because it has gravity supply tanks, a uniform diameter and composition (it is mild steel cement lined (MSCL)), and the main could be shut down for testing because a second parallel main was available. Five 9.1 ML tanks connected in series, comprising part of the summit storage at Hanson, formed an upstream boundary while a butterfly isolation valve (newly installed) could be closed, at a location known as "Sheep Dip", in order to form the 13.5 km section of transmission pipeline. Apart form these main boundaries, a 250 mm asbestos cement (AC) offtake pipe approximately 800 m long was located approximately 3.0 km from the upstream tanks. Figure 1 shows the general configuration of the HTP during the transient tests.

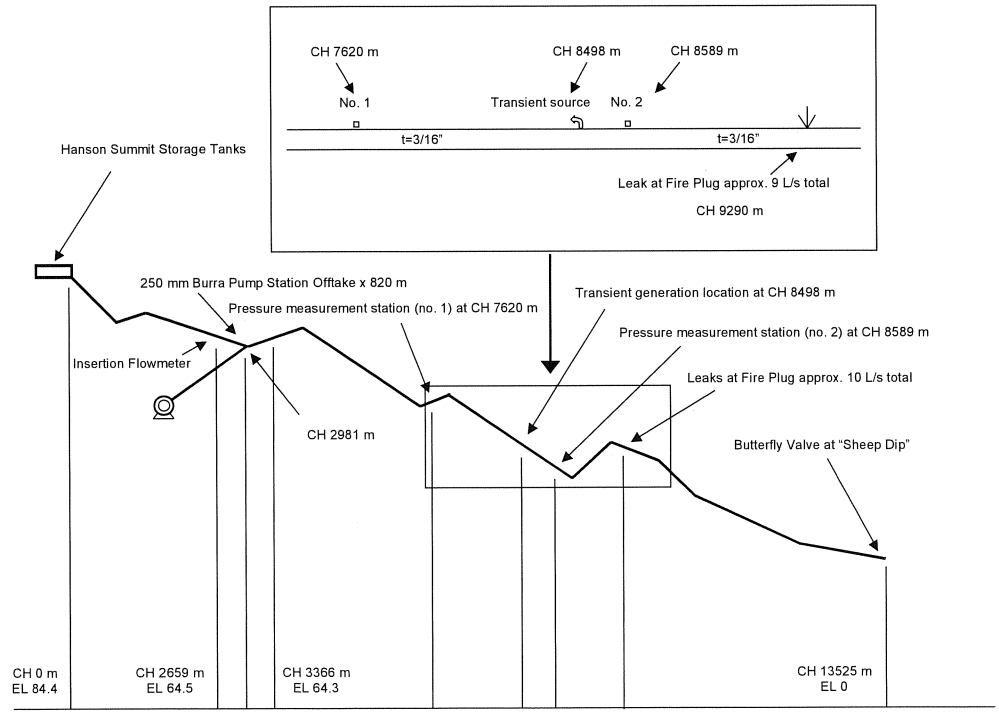

Figure 1. Test configuration for the Hanson Transmission Pipeline (HTP) (t = pipe wall thickness)

The transient source was established at chainage 8498 m from the junction immediately adjacent to the most downstream of the five 9.1 ML tanks. The method for generating the transients involved the rapid closure of a side discharge valve using the custom built device shown in Figures 5 and 6 below. Two synchronised pressure measurement stations were established at chainages 7620 m and 8589 m. These pressure measurement stations comprised a Druck PDCR-810 transducer mounted in a fitting attached to an existing air valve-fire plug location. The pressure measurement stations recorded the transient response of the HTP at 500 Hz and were synchronised using a radio tone of a known frequency that was transmitted simultaneously to both stations and recorded.

An artificial 9 L/s leak was introduced to the HTP at chainage 9290 m, to conduct transient tests without and with leakage, as described below. The discharge through the side discharge valve used to generate the transient and the leak were confirmed using an existing insertion flowmeter. Figures 2 and 3 show the chart record during the period of the tests conducted on the 21st May 2004 and the insertion flowmeter installation on the HTP. The maximum rated flow for the recorder is 450 L/s and so the percentages shown on the chart correspond with flows of approximately 43 L/s and 52 L/s for the transient tests with and without a leak, respectively. The remainder of the records from the flowmeter confirm that the flow in the HTP was reduced to approximately 0 L/s during the period between 11am and 5pm on the 21st May 2004.

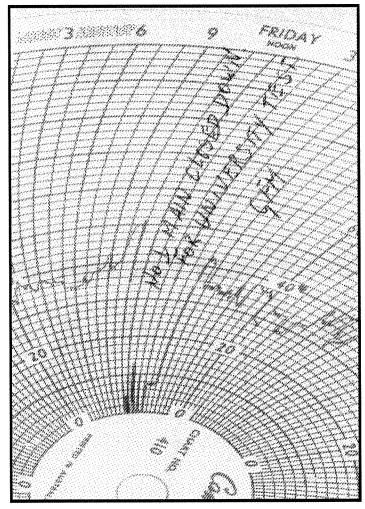

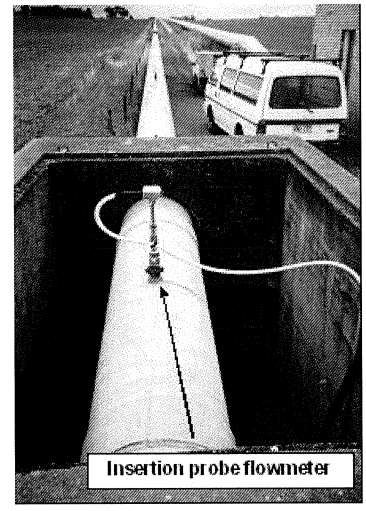

Figures 2 and 3. Detailed view of HTP chart record during the period of the tests conducted on the 21st May 2004 and a picture of the insertion flowmeter

3.2 Permissible overpressure and leak threshold

While large transient overpressures are acceptable under controlled laboratory conditions they are not acceptable on field pipelines with multiple components that may be in deteriorated condition or, alternatively, may be in a location where pressure magnification occurs such that the safe working pressure limit is exceeded. The maximum transient overpressure that the operators of water pipelines and networks will permit varies but the consensus in South Australia was that 15 m was the limit for all systems (based on discussions with operators from the South Australian Water Corporation).

South Australian Water Corporation operators considered methods for detecting leaks up to 10 L/s of interest in remote areas or along sections of pipe that were underwater or buried in porous materials. Hence, a leak of approximately this size was installed on the HTP. Figure 4 shows the leak that was installed on the HTP at the location of an existing air valve. A galvanised steel tube, 850 mm long by 55 mm diameter, was connected to the air valve and the valve opened to allow a vertical discharge. Knowing that an equivalent aperture opening of approximately 25mm existed across the seat of the valve, and taking a relatively low estimated C_d value of approximately 0.6, the C_dA_L for the leak was estimated to be approximately 0.0003 m^2. Using this C_dA_L, the approximate pressure at the location of the leak and the orifice equation the leak discharge was estimated as approximately 9 L/s. As mentioned previously, chart records from the insertion flowmeter in the HTP confirmed that an additional 9 L/s discharge occurred in the HTP when the leak was open.

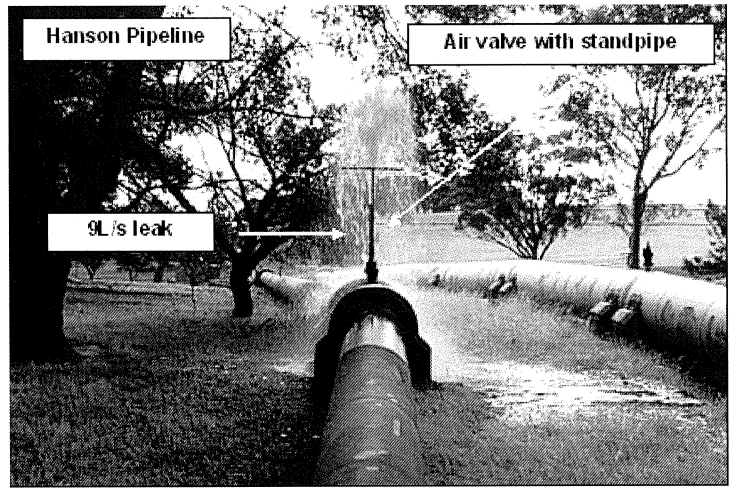

Figure 4. Simulated leak at existing air valve on the HTP

3.3 Details of artificial transient tests conducted

Controlled transients were induced in the HTP by closing a relatively large side discharge ball valve (75 mm diameter), over a period of approximately 10 ms, using the custom modified "transient generator". The speed of the closure manoeuvre was measured using a voltage potentiometer attached to the shaft of the ball valve. Figures 5 and 6 show the connection of the "transient generator" to an exiting scour valve on the HTP at the location previously shown in Figure 1. The torsion spring proved capable of closing the side discharge ball valve mounted downstream of the in-situ scour valve against a maximum differential pressure of approximately 700kPa.

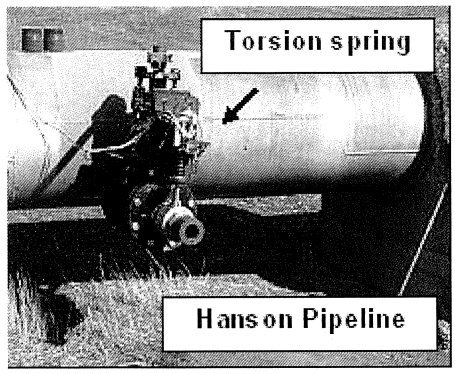

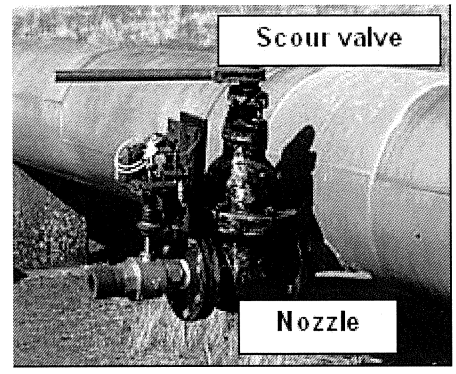

Figures 5 and 6. Torsion spring powered "transient generator" as mounted on an existing scour valve on the HTP

A set of 4 controlled transient tests were performed as described in Table 1. The controlled transients induced during tests 1 and 2 resulted in an immediate pressure rise in the HTP of approximately 7.5 m and a maximum pressure rise (above the background steady-state pressure) of approximately 15 m (tests 3 and 4 resulted in marginally smaller pressure rises). These pressures were within the operator defined allowable pressure range for the HTP.

Table 1. Summary of controlled transient tests for the HTP during May 2004

Test No.	Initial flow in main pipe	Initial velocity in main pipe	Burra pump station flow	Leak flow	Initial Reynolds No. for main pipe	Test description
1	43.0 L/s	0.140 m/s	0 L/s	0.0 L/s	76,725	No-leak test
2	43.0 L/s	0.140 m/s	0 L/s	0.0 L/s	76,725	No-leak test
3	52.0 L/s	0.169 m/s	0 L/s	9.0 L/s	92,783	Leak test
4	52.0 L/s	0.169 m/s	0 L/s	9.0 L/s	92,783	Leak test

4. FORWARD TRANSIENT AND INVERSE SOLVERS

4.1 Forward transient solver development

Covas et al. (2006) indicated that they used the Trikha (1975) approximation for unsteady friction when modelling measured responses from a 300 mm nominal diameter by 5.9 km long Scottish Water trunk main with 3-5 L/s leaks. Unfortunately, this approximation has been shown to be less accurate than those presented by, amongst others, Vitkovsky et al. (2004). This may partially account for the inability of Covas et al. (2006) to model the response of the pipeline over an extended period and thereby prevent the use the leak damping information contained in the measured responses. More significantly, as pointed out by Covas et al. (2006), boundary condition complications prevented sufficiently accurate modelling after time 2L/a seconds.

The measured responses from the HTP are not affected by boundary condition complications as described by Covas et al. (2006) because of the configuration of the pipeline with upstream tank and downstream closed valve boundaries. As a consequence, significantly less damping was observed than in the results presented by

Covas et al. (2006). Figures 7 and 8 show the comparison between the measured and predicted responses of the HTP, without any artificial leakage, when quasi-steady and then turbulent rough pipeline unsteady friction are applied with a fixed roughness of 2 mm based on CCTV camera investigation results. The turbulent rough pipe unsteady friction formulation is based on the research presented by Vardy and Brown (2004) and the efficient recursive implementation presented by Vitkovsky et al. (2004). It is apparent that the inclusion of unsteady friction improves the comparison but that a persistent discrepancy remains.

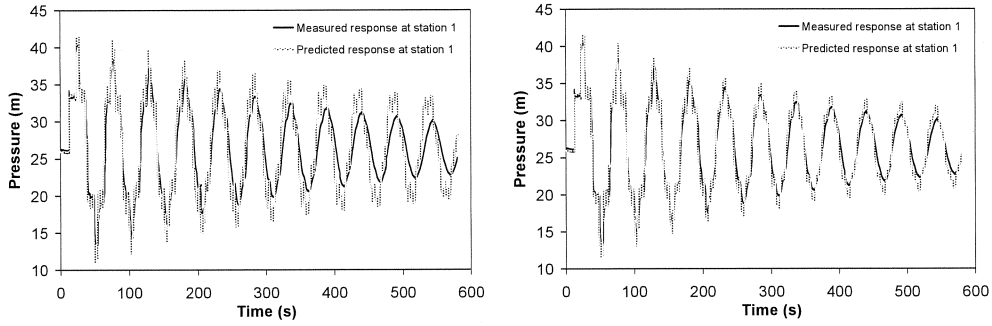

Figures 7 and 8. Comparison of measured and predicted responses for the no-leak test 1 over 600 s, at station 1, when quasi-steady (Figure 7 LHS) and unsteady friction (Figure 8 RHS) models are used with a fixed roughness of 2 mm

4.2 Inverse solver

The NLFIT suite of Bayesian non-linear regression programs has been adopted for the inverse analysis as developed by Kuczera (1994) and includes options for the application of numerous search algorithms for parameter optimization including the Levenberg-Marquardt and Genetic and Shuffled Complex Evolution – University of Arizona (SCE-UA) global algorithms. The SCE-UA global search algorithm is applied in the analysis presented below. NLFIT provides an unbiased sample variance of the residuals after fitting and an estimate of the mean and standard deviation of each model parameter (e.g., pipe roughness or "viscous" damping parameters). This information provides for a comparison between models on the basis of the fit between measured and predicted transient responses and the stability of the parameter estimates obtained following inverse fitting. The residual error is an estimate of the random error assumed by the least squares regression model and is standardised in NLFIT by dividing by the standard deviation of the residual error.

4.3 Calibration of "viscous" damping model to no-leak responses

Based on the laboratory investigations conducted by Williams (1977) and Budny et al. (1991), it is likely that the saddle supports, collar restraints and buried gullets, comprising the restraints along the HTP, together with the buried offtake branch comprising 250mm nominal diameter asbestos cement (AC) pipe with flexible joints, contribute to a significant degree of inelastic mechanical dispersion and damping. Budny et al. (1991) incorporated a "viscous" damping mechanism to account, on average, for mechanical dispersion and structural or Coulomb damping associated with the restraints for their laboratory apparatus. Williams (1977) had previously contemplated the use of an elastic hysteresis model. As for dynamic phenomena in

other fields of engineering, the use of an equivalent "viscous" mechanism, with a relatively small number of parameters, is attractive because physical complexities (e.g., complex modes of motion and vibration), and difficulties in their theoretical replication, can be avoided.

Kelvin-Voigt mechanical models can be developed to replicate "viscous" damping in many engineering applications. For pipelines subject to transients they can be applied to predict time dependent strain relaxation in the walls of plastic pipes. However, viscoelastic models have also been applied to predict the response of pipelines subject to external dynamic loads and the interaction of pipes with surrounding soils (whose behaviour can also be described as viscoelastic) by, amongst others, Rajani et al. (2004). Furthermore, the behaviour of flexible joints, as are common along pipelines, is traditionally replicated using viscoelastic or "viscous" damping. Figure 9 shows an idealised representation of the HTP and the application of two Kelvin-Voigt mechanical elements along the HTP and Burra township pump station offtake. Both the Kelvin-Voigt elements for the HTP and branch are applied uniformly at each node in an attempt to replicate the impact of the saddle supports and collar restraints along the HTP and the flexible joints and soil/pipe interaction along the buried branch, respectively.

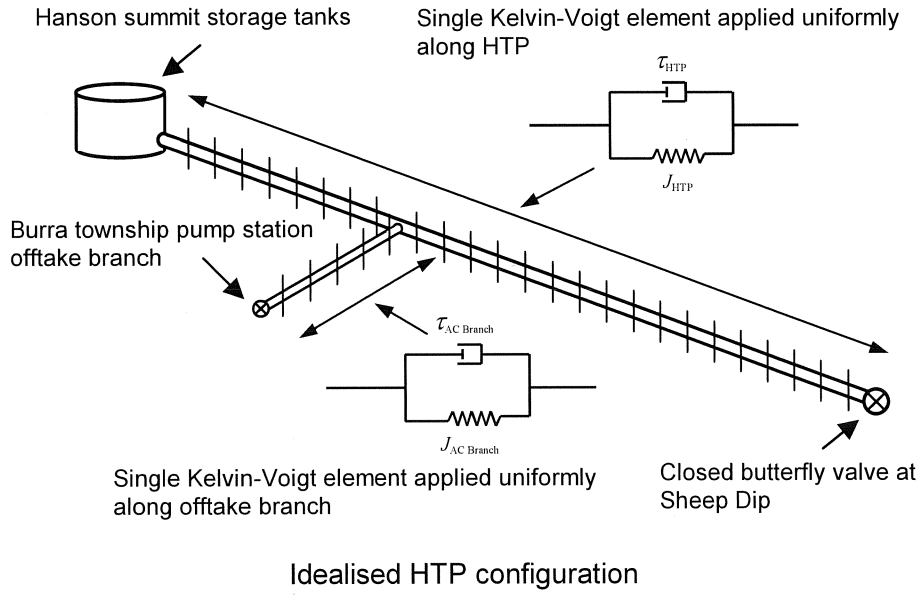

Figure 9. Schematic of the "viscous" calibration model for the HTP

In addition to the roughness in the HTP and offtake branch, Kelvin-Voigt parameters J_{HTP}, τ_{HTP}, $J_{AC\ Branch}$ and $\tau_{AC\ Branch}$, characterising the creep compliance functions in the viscoelastic model for the HTP and offtake branch, are calibrated (a total of 6 parameters need to be calibrated). The weighting functions defined by Vardy and Brown (2004), and efficient recursive implementation presented by Vitkovsky et al. (2004), are used to calculate turbulent rough pipe unsteady friction. Table 2 shows the results of the calibration for tests 1 and 2, using extended period measured responses, when unsteady friction with uniformly distributed "viscous" dispersion and damping is applied along the HTP and branch. The average fitted roughness values, for tests 1

and 2, were 5.22 mm and 4.15 mm for the HTP and offtake branch, respectively. These calibrated roughness values are greater than those estimated using two 300 m long sections of CCTV camera investigation images by are nevertheless feasible.

Table 3 shows the correlations, for test 1, between the parameters for the unsteady friction and "viscous" damping model calibrated over 600 s. All of the parameters are only weakly or moderately correlated except for J_{HTP} and the roughness for the offtake branch. This confirms that the calibration model is not over parameterised.

Table 2. Fitted HTP and branch roughness and viscoelastic parameters obtained following calibration

Fitted Parameter	TEST 1		TEST 2		Average Value of Mean μ
	Mean μ	Standard Deviation σ	Mean μ	Standard Deviation σ	
J_{HTP}	0.109e-13	0.234e-13	0.374e-13	0.205e-13	0.241e-13
τ_{HTP}	7.592	0.477e-01	6.178	0.246	6.885
$J_{ACBranch}$	0.163e-10	0.475e-12	0.142e-10	0.361e-12	0.152e-10
$\tau_{ACBranch}$	1.572	0.492e-01	1.297	0.400e-01	1.434
ε_{HTP}	0.545e-02	0.288e-03	0.499e-02	0.286e-03	0.522e-02
ε_{Branch}	0.391e-02	0.167e-01	0.439e-02	0.235e-03	0.415e-02
Objective Function	1.233		1.226		1.230

Table 3. Correlation of "viscous" parameters, and HTP and offtake branch roughness, for unsteady friction and "viscous" damping model calibration

	J_{HTP}	τ_{HTP}	$J_{AC\ Branch}$	$\tau_{AC\ Branch}$	ε_{HTP}	ε_{Branch}
J_{HTP}	1.000	0.092	-0.735	-0.524	-0.419	0.987
τ_{HTP}	0.092	1.000	-0.207	0.025	-0.232	0.064
$J_{AC\ Branch}$	-0.735	-0.207	1.000	-0.179	0.172	-0.740
$\tau_{AC\ Branch}$	-0.524	0.025	-0.179	1.000	0.443	-0.498
ε_{HTP}	-0.419	-0.232	0.172	0.443	1.000	-0.373
ε_{Branch}	0.987	0.064	-0.740	-0.498	-0.373	1.000

Figure 10 shows the comparison of the compliance function curves for the HTP and offtake branch. The "viscous" damping is greater per pipe sub-segment (approximately 20 m) along the offtake branch, and contributes more rapidly to the calibrated response, relative to the effect along the HTP. The compliance function curve derived from the calibrated J_{HTP} and τ_{HTP} parameters has a less significant damping effect per pipe sub-segment and is slower acting (i.e., the full "creep" values do not apply until after time 16 s). However, the cumulative impact of the calibrated "viscous" damping is significant along the length of the HTP.

Figures 11 and 12 show the comparison, at station 1, between measured and predicted responses for test 1, after calibrating using the unsteady friction and "viscous"

damping model, over 600 s and 100 s, respectively. The calibration, for tests 1 and 2, gives an average objective function of 1.230. It is apparent that the comparison between the measured and predicted responses is significantly improved relative to those obtained using quasi-steady and unsteady friction models without "viscous" damping. That said, Figure 12 shows that the measured dispersion over the initial response is not exactly replicated by the predicted response.

The approximation of the inelastic dispersion and damping using an equivalent "viscous" mechanism, and the consequent loss of distinct "structure" in the predicted response, makes it difficult to independently fit multiple parameters representing different physical complexities affecting the measured response of the HTP (e.g., roughness and restraint effects). However, the accuracy of the forward model is significantly greater than that presented by Covas et al. (2006). Furthermore, it facilitates inverse transient analysis (ITA) that makes use of both reflection and damping information as originally envisaged by Liggett and Chen (1994).

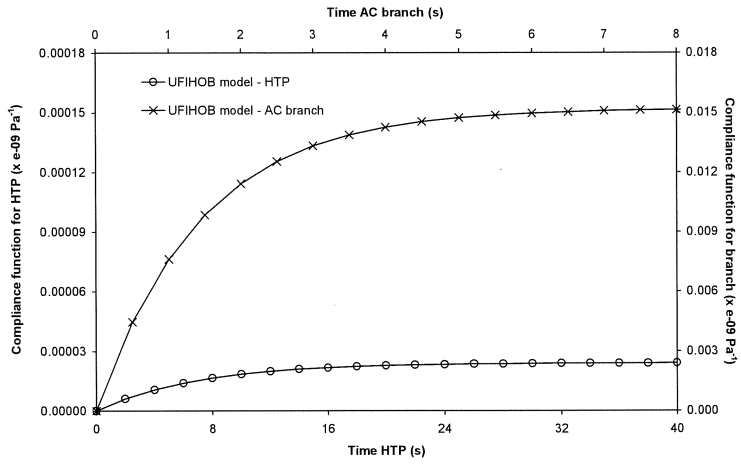

Figure 10. Comparison of compliance function curves for HTP and AC branch following calibration of "viscous" damping model using measured responses

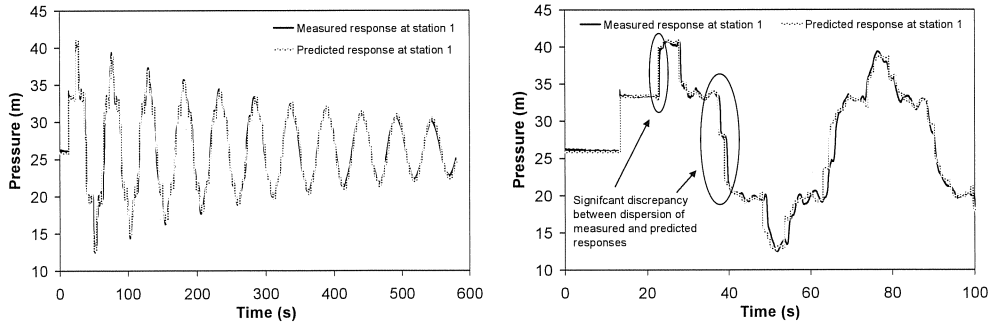

Figures 11 and 12. Comparison of measured and predicted responses, at station 1, for test 1 using calibrated unsteady friction and "viscous" damping model over 600 s and 100 s, respectively

5. RESULTS OF ANALYSIS USING REFLECTION INFORMATION

5.1 Indistinctiveness of measured leak reflection information

Figures 13 and 14 show the measured leak reflections for test 3 at stations 1 and 2, respectively. The predicted leak reflections, respectively 0.108 m and 0.110 m, are superimposed for the purpose of comparison. A marginal fall in the measured response is discernable at the location of the leak. The average measured pressures for 0.5s prior to and following the time of the leak reflection for test 3 at station 1 are 33.092 m and 32.989 m giving an average drop of 0.103 m. For station 2, the average measured pressures are 61.789 m and 61.693 m giving an average drop of 0.096 m. The results confirm that, for the size of leak and maximum permissible overpressure specified by South Australian system operators, small leak reflections occur in larger transmission pipelines.

Furthermore, the leak reflections are difficult to discern amongst background hydraulic noise. The results for Covas et al. (2006) stand in stark contrast but can be explained by the fact that the pipeline tested was only 300 mm in diameter, had a very high static head (132 m) and was subjected to an overpressure of 13.2 m. The sources of the hydraulic noise include flow variability or "flutter" through the nozzle mounted in the "transient generator", interaction of the relatively sharp wavefronts with wall lining (and wall) thickness and other material variations and reflections from the saddle supports and collar restraints. Unfortunately, for leak sizes around the threshold of interest, the measured reflections are within the hydraulic noise band giving a very low leak signal to hydraulic noise ratio.

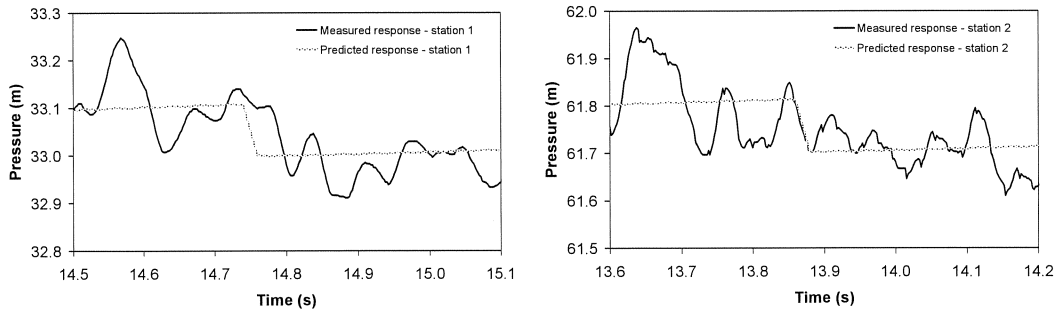

Figures 13 and 14. Measured versus predicted leak reflections for test 3 at stations 1 and 2, respectively

5.2 ITA using unsteady friction and "viscous" damping model for 2L/a seconds

In a similar fashion to Covas et al. (2006), ITA has been performed with the analysis limited to the first 2L/a seconds of the measured response of the pipeline. However, in contrast to the results presented by Covas et al. (2006), a turbulent rough pipe unsteady friction calculation with calibrated "viscous" damping will be used. The calibration has been performed over 2L/a seconds to match the length of time for the ITA using the no-leak responses for tests 1 and 2 in a similar manner to that described previously.

Figures 15 and 16 show the logarithm of the ratios between the objective functions determined for each potential leak location and the minimum objective function obtained when ITA is performed by fixing the leak location at individual nodes along the HTP and then fitting for the optimum leak size, without and with prior information regarding the leak discharge, respectively. The potential leak locations are spaced 40 nodes apart (approximately 800 m). This spacing is coarser than that used by Covas et al. (2006) and the approach outlined in their paper could be applied to attempt to further refine the identification of the leak location. However, for the purposes of this paper this was not necessary.

Figure 15 shows that, without prior information regarding the leak discharge, the minimum objective function is obtained when the leak location is fixed at node 241. The objective function when the leak is fixed at its "true" location (node 441) is ranked 5th from the minimum value for the leak at node 241. There is a significant difference between the fitted leak sizes, at nodes 241 and 441, of 0.000649 m^2 and 0.000365 m^2, respectively. The fitted leak size at node 441 is closer to the "true" leak size of 0.0003 m^2. Figure 16 shows that, with prior information regarding the leak discharge, the minimum objective function is obtained when the leak location is fixed at node 321. The objective function when the leak is fixed at its "true" location (node 441) is ranked 3rd from the minimum value.

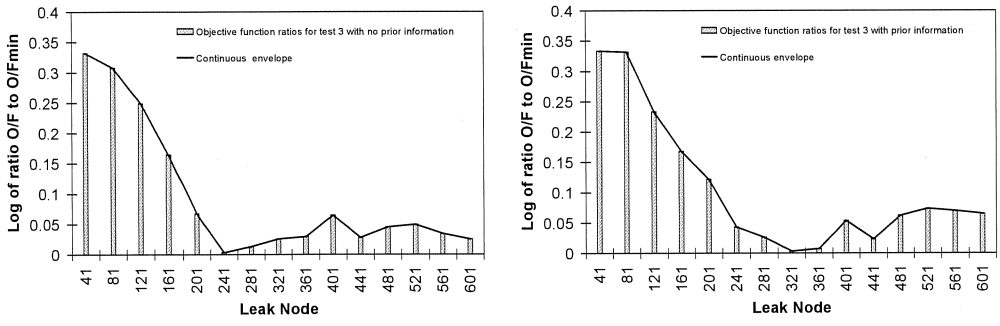

Figures 15 and 16. Using the "viscous" damping model to perform ITA, over 2L/a seconds, for test 3, without and with prior information, respectively

Figures 17 and 18 show the measured and predicted responses at station 1, over a time scale of 2L/a seconds, for the leak at its "true" location (node 441), when ITA is performed without and with prior information regarding the leak discharge, respectively. An erroneous leak size of 0.000365 m^2 is fitted when ITA is performed without prior information regarding the "true" leak size. The magnitude and timing of the measured and predicted incident transient wavefront, reflections from the closed in-line valve and tanks and reflections from the offtake branch compare reasonably. That said, the small leak reflections, shown in the insets in both figures, are not of a sufficient magnitude for the 9 L/s leak to significantly influence the ITA and therefore do not facilitate the accurate location or sizing of the leak when either the location and/or size of the leak are not pre-specified.

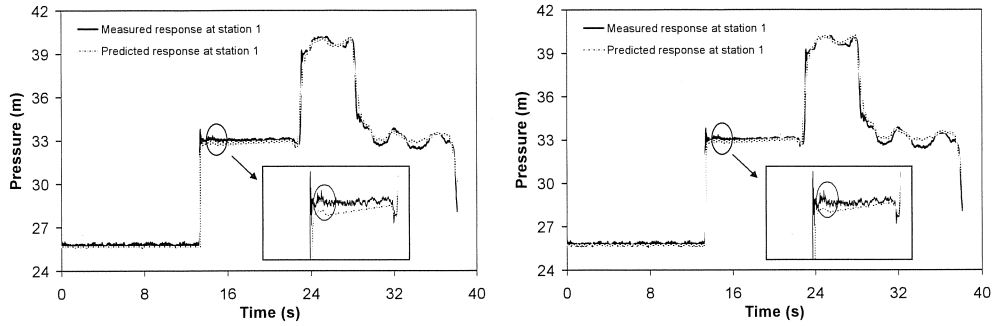

Figures 17 and 18. Measured and predicted responses at station 1 when the leak is located at node 441, and ITA is performed over 2L/a seconds, using the "viscous" damping model, without and with prior information, respectively

6. RESULTS OF ANALYSIS USING DAMPING INFORMATION

The results presented above contrast starkly with those presented by Covas et al. (2006). The explanation lies in a combination of factors including the fact that the HTP is 650 mm nominal diameter whereas the Scottish Water pipeline tested by Covas et al. (2006) was only 300 mm in diameter. While the leaks introduced by Covas et al. (2006) were 3-5 L/s and smaller than the 9 L/s leak introduced to the HTP the relationship between pipeline and leak size is not linear.

Where leak reflection information is indistinct, and cannot be effectively used for leak location and sizing, the possibility of using leak damping information over an extended period remains. However, as emphasised above, an accurate forward transient model is required and dispersion and damping not related to the leak must be isolated. The numerical investigation presented by Liggett and Chen (1994) utilised both reflection and extended period damping information because the forward model was able to accurately replicate the numerically generated "measurement" data. For field pipelines, numerous physical uncertainties contribute to damping that is not related to leakage and this damping needs to be isolated if leak damping information is to be used to complement leak reflection information and facilitate successful diagnosis. The unsteady friction and "viscous" damping model described above, as calibrated to the no-leak responses, is applied below to determine whether the extended period damping information in the measured responses for the HTP can be used for ITA to successfully locate and size the known 9 L/s leak.

6.1 ITA using quasi-steady friction model over 600s

Before applying the unsteady friction and "viscous" damping model the results of analysis performed using a quasi-steady model over an extended period will be presented for the purpose of comparison. Figure 19 shows that, without prior information regarding the leak discharge, the minimum objective function is obtained when the leak location is fixed at node 401. The objective function when the leak is fixed at its "true" location (node 441) is ranked 6th from the minimum value for the leak at node 401. There is a significant difference between the fitted leak sizes, at nodes 401 and 441, of 0.000527 m^2 and 0.000474 m^2, respectively. The fitted leak size at node 441 is closer to the "true" leak size of 0.0003 m^2. Figure 20 shows that,

with prior information regarding the leak discharge, the minimum objective function is obtained when the leak location is fixed at node 361. The objective function when the leak is fixed at its "true" location (node 441) is ranked 3rd from the minimum value. This represents an improvement relative to the results obtained without prior information regarding the leak discharge.

Figures 21 and 22 show the measured and predicted responses at station 1, over a time scale of 600s, for the leak at its "true" location (node 441), when ITA is performed without and with prior information regarding the leak discharge, respectively. Figure 21 confirms that the quasi-steady friction model does not replicate non-leak related dispersion particularly accurately. However, the measured damping is approximately replicated because of an erroneously fitted leak size of 0.000474 m^2 (compared to the "true" C_dA_L of 0.0003 m^2). Figure 22 shows that, by fixing the leak size to its "true" value, the measured damping cannot be replicated by inaccurately calibrating for the size of the leak.

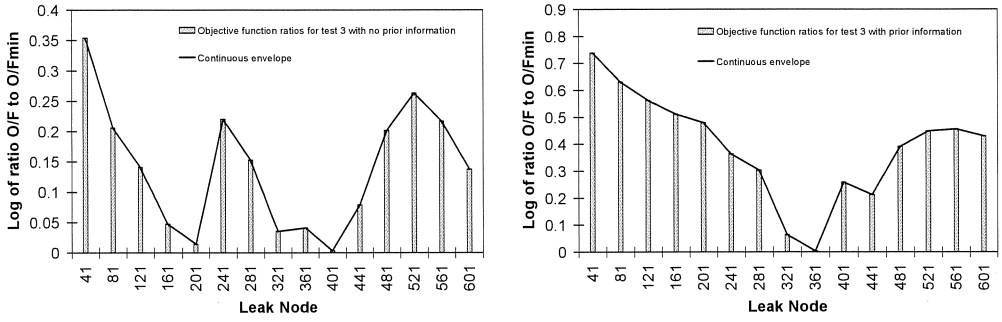

Figures 19 and 20. Using the quasi-steady friction model, calibrated over 600 s, to perform extended period ITA for test 3, without and with prior information, respectively

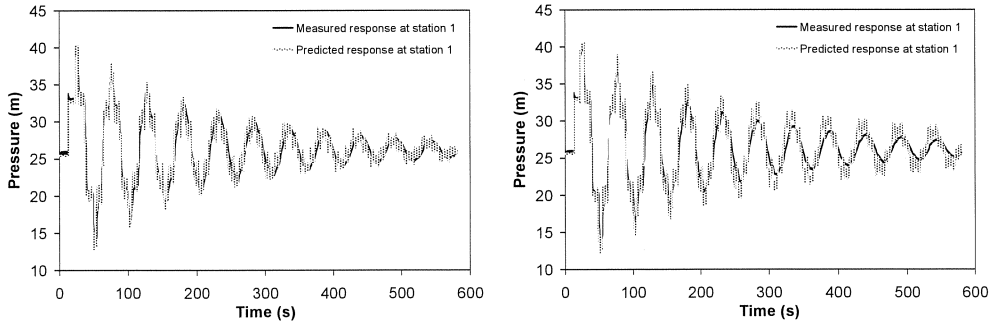

Figures 21 and 22. Comparison between measured and predicted responses at station 1, over 600 s, when the leak is located at node 441, and ITA is performed without and with prior information, respectively

6.2 ITA using unsteady friction and "viscous" damping model over 600 s

ITA has been performed using the unsteady friction and "viscous" damping model to locate and size the artificially introduced 9 L/s leak using the extended period measured responses for tests 3 and 4. Figure 23 shows that, without prior information regarding the leak discharge, the minimum objective function is obtained when the

leak location is fixed at node 201. The objective function when the leak is fixed at its "true" location (node 441) is ranked 8th from the minimum value for the leak at node 201. This represents a deterioration relative to the results obtained using the quasi-steady friction model. There is a significant difference between the fitted leak sizes, at nodes 201 and 441, of 0.000768 m^2 and 0.000328 m^2, respectively. The fitted leak size at node 441 is close to the "true" leak size of 0.0003 m^2. Figure 24 shows that, with prior information regarding the leak discharge, the minimum objective function is obtained when the leak location is fixed at node 321. The objective function when the leak is fixed at its "true" location (node 441) is ranked 2rd from the minimum value. This represents an improvement relative to the results obtained without prior information regarding the leak discharge and to those obtained using the quasi-steady friction model.

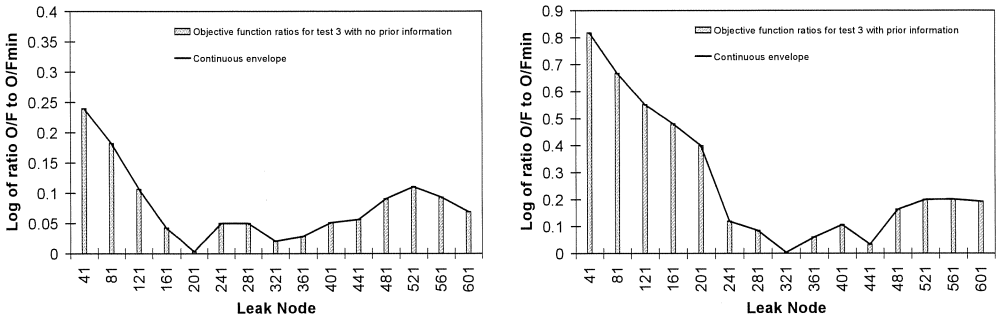

Figures 23 and 24. Using the unsteady friction and "viscous" damping model, calibrated over 600 s, to perform extended period ITA for test 3, without and with prior information, respectively

Figures 25 and 26 show the measured and predicted responses at station 1, over a time scale of 600 s, for the leak at its "true" location (node 441), when ITA is performed without and with prior information regarding the leak discharge, respectively. The replication of the measured response is marginally improved when an erroneous leak size of 0.000328 m^2 is fitted. As for the results obtained using the quasi-steady friction model, this indicates that the fitted leak size is acting to compensate for non-leak related damping rather than any error with the fixed leak size of 0.0003 m^2. In fact, constraining the leak size to match the known discharge increases the relative difference between the measured and predicted responses, for each potential leak location, unless the leak is fixed at its "true" location. Hence, the use of prior information regarding the leak discharge, from flow monitoring records (if available), will always improve the result of any ITA and eliminate erroneous matches achieved with incorrectly fitted parameters.

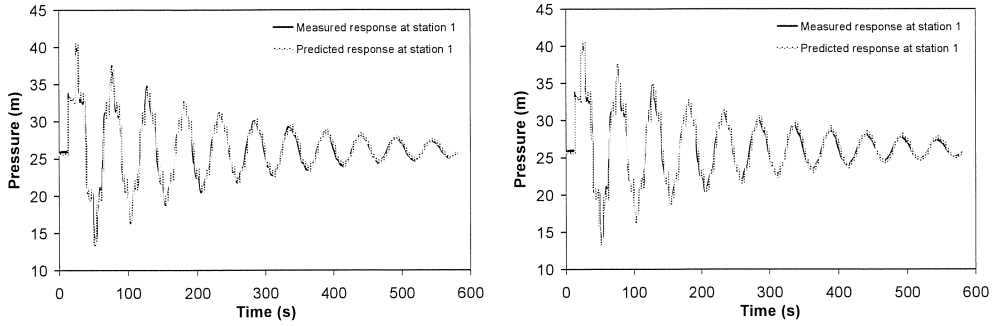

Figures 25 and 26. Comparison between measured and predicted responses at station 1, over 600 s, when the leak is located at node 441, and ITA is performed without and with prior information, respectively

7. CONCLUSIONS

The field tests conducted on the HTP as reported in this paper confirm that leaks do affect the transient response of a pipeline and in this regard they are possible to detect. This confirms the observations made by Covas et al. (2006). However, the results provide an important comparison relative to those presented by Covas et al. (2006) and show that while discernable leak reflections may be obtained in the first 2L/a seconds of a transient response for smaller pipelines, which are sufficient to enable leak location and sizing using inverse procedures, leak reflections on larger pipelines, such as the HTP, are likely to be much less discernable and partially obscured by non-leak related reflections.

Given the indistinctiveness of the direct leak reflection information, improved transient models have been applied to more accurately replicate the measured responses from the HTP and thereby facilitate the use of leak damping information for leak diagnosis. Turbulent rough pipe unsteady friction has been incorporated in the modelling as well as a "viscous" damping mechanism to account for dispersion and damping caused by mechanical motion and vibration. This "viscous" damping model was then calibrated to measured no-leak responses from the HTP to obtain suitable parameter estimates.

The forward transient modelled was then applied to perform ITA as originally envisaged by Liggett and Chen (1994) whereby the information, both reflections and damping, from the entire measured responses from the HTP was used. Unfortunately, while the leak damping information was clearly discernable, it could not be satisfactorily isolated from the non-leak related sources of damping, using the "viscous" damping model, with the consequence that the location and size of the leak could not be accurately determined. That said, the use of prior information regarding the leak discharge compensated for the deficiencies in the forward transient model such that the leak was identified as the 2nd or 3rd ranked candidates when extended period ITA was performed. Developing a greater understanding of transient reflections from non-leak related sources and the influence of these upon extended period damping is required if the accuracy with which leaks are located and sized using ITA is to be further improved.

8. ACKNOWLEDGEMENTS

The authors gratefully acknowledge the financial support of the Australian Research Council, and the field support of operators from the South Australian Water Corporation, for the research reported above.

9. REFERENCES

Budny D., Wiggert D. C. and Hatfield F. J. (1991) "The influence of structural damping on internal pressure during a transient pipe flow" Journal of Fluids Engineering ASME 113(3), 424-429

Covas D., Ramos H., Lopes N. and Almeida A. B. (2006) "Water pipe diagnosis by transient pressure signals" 8th Annual Water Distribution Systems Analysis Symposium, Cincinnati, Ohio, U.S.A., August 27-30, 2006

Kuczera G. (1994) "NLFIT : A Bayesian Nonlinear Regression Program Suite" University of Newcastle, New South Wales, Australia

Liggett J. and Chen L. C. (1994) "Inverse transient analysis in pipe networks" Journal of Hydraulic Engineering ASCE 120(8), 934-955

Rajani B. and Tesfamariam S. (2004) "Uncoupled axial, flexural and circumferential pipe-soil interaction analyses of partially supported jointed water mains" Canadian Geotechnical Journal 41, 997-1010

Trikha A. K. (1975) "An efficient method for simulating frequency-dependent friction in transient liquid flow" Journal of Hydraulic Engineering ASCE 97(1), 97-105

Vitkovsky J., Stephens M., Bergant, A., Lambert, M. and Simpson, A. (2004) "Efficient and accurate calculation of Zielke and Vardy-Brown unsteady friction in pipe transients" 9th Int. Conf. On Pressure Surges, Chester, UK, BHR Group, Cranfield, U.K., 405-419

Vardy A. and Brown J. (2004) "Efficient approximation of unsteady friction weighting functions" Journal of Hydraulic Engineering ASCE 130(11), 1097-1107

Williams D. J. (1977) "Waterhammer in non-rigid pipes: precursor waves and mechanical damping" Journal of Mechanical Engineering Science ASME 19(6), 237-242